Entropy of Polymer Brushes in Good Solvents: A Monte Carlo Study

Kaoru Ohno,*,† Takashi Sakamoto,† Taisuke Minagawa,†,‡ and Yutaka Okabe§

Department of Physics, Yokohama National University, 79-5 Tokiwadai, Hodogaya, Yokohama 240-8501, Japan; Department of Physics, Purdue University, West Lafayette, Indiana 47907; and Department of Physics, Tokyo Metropolitan University, 1-1 Minamiosawa, Hachioji, Tokyo 192-0397, Japan

Received June 13, 2006; Revised Manuscript Received November 22, 2006

ABSTRACT: Entropy of polymer brushes composed of monodisperse flexible polymer chains regularly grafted on a flat substrate plane with an equal "*spacing*" is numerically studied in the good solvent limit. We consider systems of not only a free polymer brush but also a compressed polymer brush and two polymer brushes facing each other at a "*distance*". The total number of configurations, entropy, and force are calculated for various chain lengths and graft densities by means of Monte Carlo simulations using an efficient enrichment algorithm on a simple cubic lattice. We demonstrate that the effect of excluded volume plays an essential role. We find that the entropy of a free polymer brush falls as $-\Delta S \sim (spacing)^{-2.4\pm0.1}$, while the entropy of a compressed polymer brush and two polymer brushes agrees very well with the analytical SCF theory by Milner, Witten, and Cates [*Macromolecules* **1988**, *22*, 2610−2619]. The resulting interlayer force agrees also excellently well with the recent experiments by Yamamoto et al. [*Macromolecules* **2000**, *33*, 5602−5607].

I. Introduction

The systems composed of many monodisperse polymer chains end-grafted regularly on a flat substrate plane, which are called polymer brushes or polymer layers, have attracted considerable interest because the synthesis of polymer brushes with high graft densities has become possible with a controlled fashion.[1−9] It has been observed experimentally that one polymer brush compressed by a flat wall parallel to the brush substrate or two polymer brushes facing each other repel strongly as the two layers approach in good solvents, despite the mutual van der Waals attractions between polymers.[1−5] This effect is due to the large osmotic repulsions between segments in the opposing layers and has been used in the steric stabilization of colloidal dispersions.[1,2] Taunton et al.[3] measured in their pioneering work the force−distance dependence of two polymer brushes swollen in good solvents. More recently, Yamamoto et al.[4,5] performed a similar experimental study of polymer brushes with relatively high graft densities. They demonstrated that polymer brushes with high graft densities are much more stretched than those with moderate graft densities. The concentration profile of a polymer brush swollen in good solvents has been extensively studied also.[6,7] The property of polymer brushes changes according to the flexibility, the hydrophilicity, the length, and the graft density of the chains as well as the property of the solvent. They are mutually repulsive, soft, cushiony, sleek, and lubricate or, alternatively, sticky and adhesive. The repulsive, soft, and lubricative (or cushionlike) properties of polymer brushes purely come from the entropic force due to the excluded-volume effect among polymer chains, while their sticky and adhesive properties come from the entanglement effects. These properties are also of fundamental importance because all these effects are absent in the systems of ideal chains without the excluded-volume effect. They appear only in the systems of real chains that have the excluded-volume effect.

Also, a lot of theoretical investigations have been performed on the free energy or the entropy in the case of good solvents of the polymer brush systems, from which the force acting on the layers can be derived. The entropy was first treated with Flory−Huggins mean-field theory combined with a scaling theory by Alexander[10] and de Gennes,[11] who assumed a step-function-like concentration profile. A more elaborated self-consistent-field (SCF) theory of the grafted polymer brush was proposed by Scheutjens and Fleer.[12] The SCF equation was solved numerically by Cosgrove et al.[13] and Muthukumar and Ho.[14] It was also solved analytically by Milner, Witten, and Cates[15] in the limit of high molecular weight, who obtained parabolic form for the concentration profile. According to their analytic theory, the universal form for the free energy of the polymer brush systems is expressed as

$$F \sim \frac{1}{2u} + \frac{u^2}{2} - \frac{u^5}{10} \tag{1}$$

where $u = (distance)/(nh^*)$ and n is the number of polymer brushes ($n = 1$ for a compressed polymer brush and $n = 2$ for two facing polymer brushes), *distance* denotes the interplane distance, and h^* denotes the equilibrium height of the corresponding free polymer brush. Hereafter we will refer this analytical free energy as the MWC theory. A related but somewhat different analysis was independently given by Zhulina et al.[16] Then, a lot of theoretical and numerical works have been reported on this subject. Murat and Grest performed a molecular dynamics study of a grafted polymer brush[17] and two brushes[18] and compared their result of the monomer concentration profile with the SCF theory. Their numerical result for intermediate values of surface coverage agrees well with the analytic form derived by Milner et al. but deviates qualitatively from it for higher values of surface coverage. Monte Carlo simulations of a polymer brush were first carried out by Lai and Binder,[19] who investigated the concentration profiles and dynamical properties as a function of the chain length and the graft density. They also investigated a polymer brush in the Θ solvent[20] as well as a polymer brush under shear.[21] The force between two grafted

† Yokohama National University.
‡ Purdue University.
§ Tokyo Metropolitcan University.
* Corresponding author: e-mail: ohno@ynu.ac.jp.

10.1021/ma0613234 CCC: $37.00
Published on Web 01/09/2007

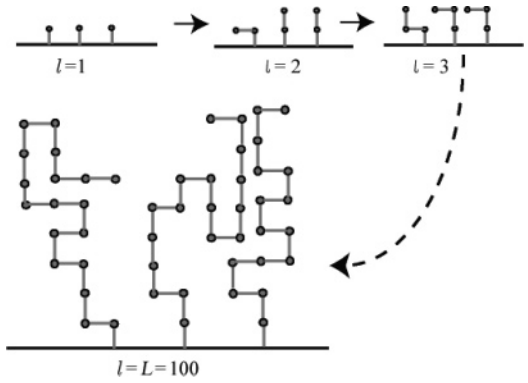

Figure 1. Schematic illustration of the enrichment algorithm.

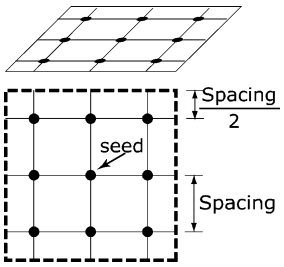

Figure 2. Polymer chains are grafted regularly in a square lattice at the points indicated by "seed". The lattice constant (i.e., the nearest-neighbor distance of grafted points) is called "*spacing*." The periodic boundary condition is used in the directions parallel to the substrate planes.

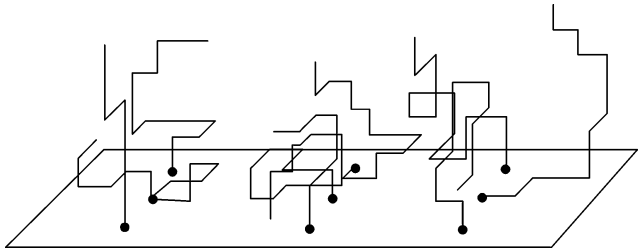

Figure 3. Schematic illustration of the system geometry of a free polymer brush.

polymer brushes was investigated in terms of Monte Carlo simulations by Dickman and Anderson[22] and by Toral et al.[23] They compared their result with the MWC theory of the analytic SCF force (i.e., the derivative of eq 4 with respect to the *distance*). The agreement between their numerical result and the MWC theory was good but not perfect. More recently, using a molecular dynamics simulation, Kreer et al. investigated the applicability of the SCF theory[24] and the force vs distance curves of brushes against each other.[25]

The aim of this paper is to investigate directly the entropy or equivalently the free energy in the good solvent limit of the system of not only a free or compressed polymer brush but also two polymer brushes facing each other by carrying out an extensive Monte Carlo simulation and to show that the agreement between the resulting entropy and the MWC theory is perfect. In the good solvent limit, configurations of polymers become energy independent provided that configurations with overlaps of polymers are not allowed, and the free energy is identical to the entropy with a minus sign. Here we use the lattice Monte Carlo simulation using the enrichment algorithm[26−30] which can count efficiently the total number of configurations of multipolymer systems and in turn their entropy. As explained above, the entropy is of fundamental interest because its derivative gives a force due to the effect of purely excluded

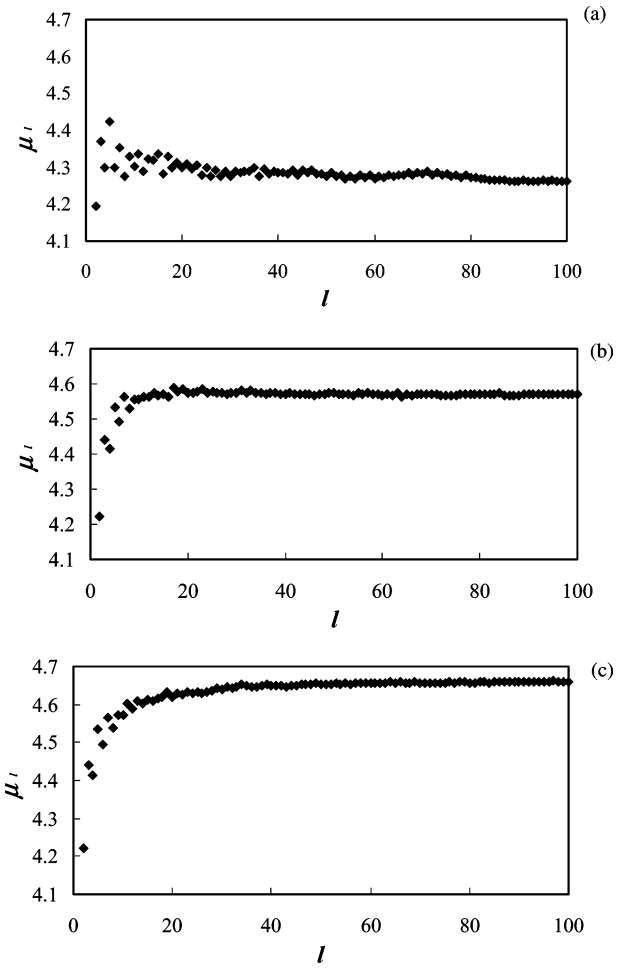

Figure 4. Effective coordination number μ_l as a function of the chain length l in the case of one polymer brush: (a), (b), and (c) correspond to *spacing* = 4, 8, and 20, respectively.

volume. Note that no such force exists without this effect. The quantity should have a quantitative relation to the spacing between grafted points and the chain length. In the system of a compressed polymer brush or two polymer brushes, the distance between the two planes becomes an additional important quantity. Then the interlayer force is governed by the derivative of the entropy with respect to the distance. This is the first-time direct Monte Carlo study of the entropy of these systems.

The rest of this paper is organized as follows. In section II, we describe the methodology of the present simulation algorithm. The results of one- and two-brush systems are presented respectively, in sections IIIA and IIIB. Finally, section IV concludes this paper.

II. Methodology

So far, we have successfully applied an efficient enrichment Monte Carlo method on a simple cubic lattice to the systems of one or two star polymers[26−29] and polymer solutions at dilute and semidilute regimes.[30] First, we briefly describe this enrichment algorithm. The principle of the algorithm is to generate the configurations of monodisperse long chains by elongating all chains stepwise (see Figure 1). Suppose that the system consists of F chains with the same length l; i.e., they are composed of the same number l of the segments. We refer these configurations to as the lth generation samples. At each step of the simulation, we elongate the length of each chain by one by adding one segment to each end of the chains and make the

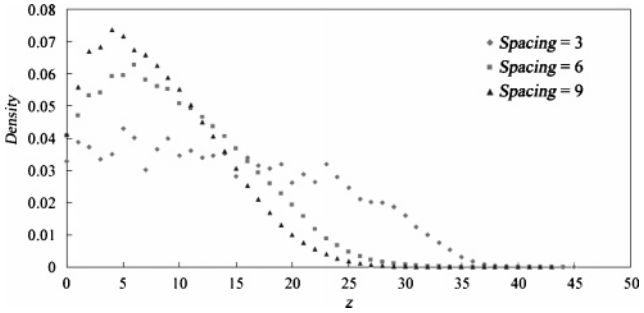

Figure 5. Density profile of free polymer brushes with *spacing* = 3, 6, and 9. The chain length is $L = 100$.

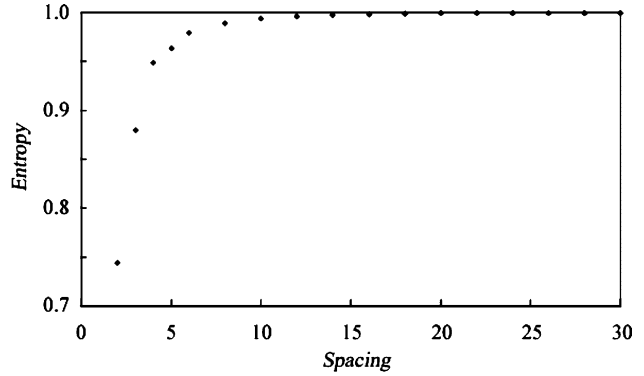

Figure 6. Entropy of the system of a free polymer brush as a function of *spacing*. The ordinate is normalized by the value of the entropy S_∞ at infinite *spacing*.

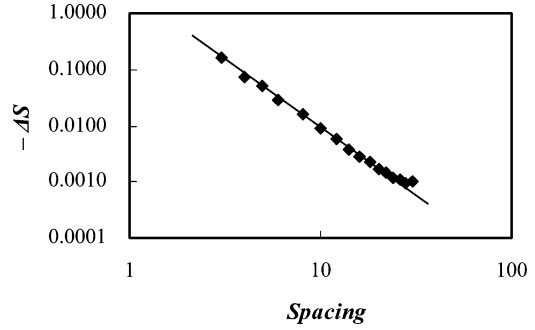

Figure 7. Double-logarithmic plot of the entropy change $-\Delta S = S_\infty - S$ as a function of *spacing*. Its slope -2.4 ± 0.1 corresponds to the exponent $-x$ in eq 3.

$(l + 1)$th generation from the lth generation. The direction of elongations is chosen randomly, excluding the direction that would fold backward. Some of the newly generated samples may violate the excluded-volume condition. Such configurations are simply eliminated. By repeating this procedure until the length of each chain reaches the target length L, we can generate a large number of samples of the monodisperse chains satisfying the excluded-volume condition.

The merit of this enrichment algorithm is that it can directly estimate the ratio of the total number of configurations of the lth generation, $N(l)$, to that of the $(l - 1)$th generation, $N(l - 1)$, from the success ratio $p(l)$ of a Monte Carlo attempt of elongating all chains simultaneously by one segment. They are related to each other through the relation

$$\frac{N(l)}{N(l-1)} = p(l)(z-1)^F = \mu_l^F \qquad (2)$$

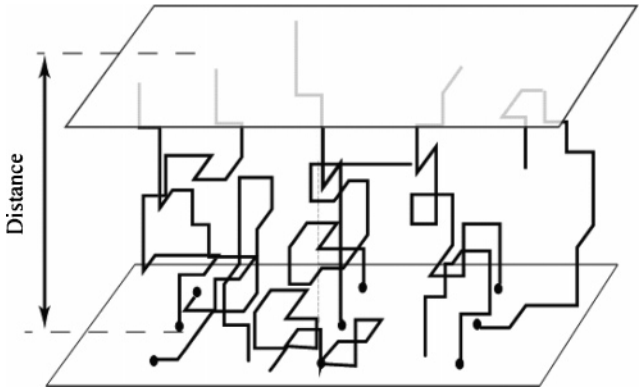

Figure 8. Schematic illustration of the system geometry of a compressed polymer brush. Here, "*distance*" denotes the distance between the brush substrate plane and the upper plane.

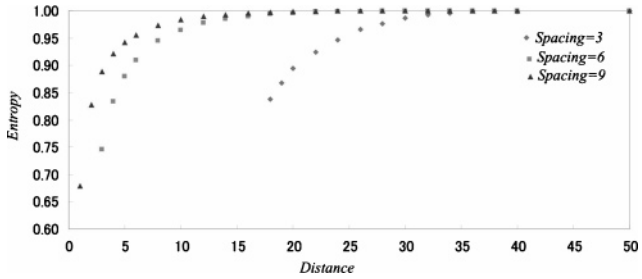

Figure 9. Entropy of the system of a compressed polymer brush. The ordinate is normalized by the value of the entropy at infinite *distance*. The results for three systems with *spacing* = 3, 6, and 9 are shown.

where z (=6) and μ_l denote respectively the true and effective coordination numbers of the simple cubic lattice. The number $z - 1$ comes from the number of possible attempts of elongating one chain provided that we do not elongate the chain backward to fold on itself. In a system of one isolated chain, μ_l is known to approach 4.6838... in the limit $l \to \infty$.[31] Thus, the ratios $N(l)/N(l-1)$ can be obtained for all chain lengths $l = 2$ to L within one simulation run. Multiplying these ratios, we can derive the desired total number of configurations $N(L)$ by

$$N(L) = \frac{N(L)}{N(L-1)}\frac{N(L-1)}{N(L-2)}\cdots\frac{N(3)}{N(2)}\frac{N(2)}{N(1)}N(1) \qquad (3)$$

The last factor $N(1)$ is the number of the possible first-generation samples, which amounts to the number of the ways to place F segments at the seed points. The seed points are regularly distributed on a substrate plane. The algorithm is applicable to the system of two polymer brushes as well. In that case, the elongation starts from the F points regularly distributed on two parallel planes.

From eq 3, we can determine the dimensionless entropy via the relationship $S = \log N(L)$. Since the system is assumed as athermal solution in the good solvent limit, we simply disregard the configuration dependence of the energy and simply set $k_BT = 1$; hence, the free energy becomes dimensionless and is given by $-\log N(L)$. From this, one can calculate force acting on the system.

In the present simulation, a square cell and a periodic boundary condition are employed in the directions parallel to the substrate plane(s). Inside a unit cell, a polymer brush is composed of 3×3 (=9) polymer chains end-grafted at the seed points equally separated with a length designated by "*spacing*" on a substrate plane, as illustrated in Figure 2. The system of

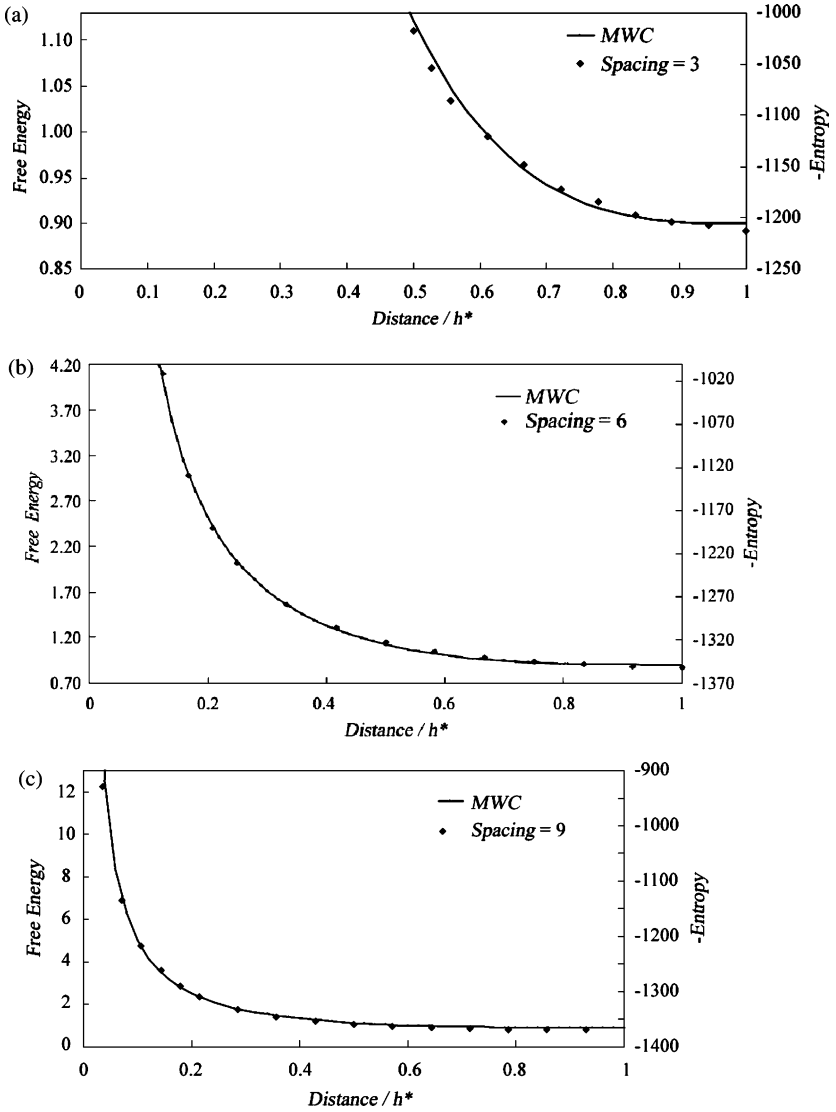

Figure 10. Comparison between the present result for the negative entropy (dots) and the MWC theory for the free energy (solid curves) in the case of a compressed polymer brush.

Table 1. Entropy and the Lateral Linear Dimensions of a Compressed Polymer Brush with a Larger Number ($F = 16 = 4 \times 4$) of Polymers Grafting on a Substrate for Several Sets of *Spacing* and *Distance*[a]

spacing	*distance*	entropy $S(16)$	entropy $S(9)$	$S(16)/S(9)$	$\sqrt{\langle x^2+y^2\rangle_g}$	$\sqrt{\langle x^2+y^2\rangle_e}$
3	20	1948 ($L = 100$)	1074 ($L = 100$)	1.813	6.9 ± 0.6	10.2 ± 0.9
3	28	2116 ($L = 100$)	1184 ($L = 100$)	1.787	6.1 ± 0.5	8.5 ± 1.0
3	40	2146 ($L = 100$)	1211 ($L = 100$)	1.771	6.1 ± 0.5	9.4 ± 0.8
3	50	2128 ($L = 100$)	1204 ($L = 100$)	1.767	6.5 ± 0.5	8.8 ± 0.6
6	3	1506 ($L = 75$)	842 ($L = 75$)	1.789	6.1 ± 0.5	8.2 ± 0.6
6	6	2182 ($L = 100$)	1229 ($L = 100$)	1.775	8.4 ± 0.7	12.0 ± 1.3
6	10	2322 ($L = 100$)	1306 ($L = 100$)	1.778	8.6 ± 0.5	12.4 ± 1.1
6	20	2396 ($L = 100$)	1349 ($L = 100$)	1.776	7.7 ± 0.5	11.2 ± 1.1
6	32	2359 ($L = 100$)	1352 ($L = 100$)	1.771	8.1 ± 0.6	11.8 ± 1.3
9	3	2162 ($L = 100$)	1216 ($L = 100$)	1.778	7.9 ± 0.5	10.5 ± 1.5
9	6	2328 ($L = 100$)	1309 ($L = 100$)	1.778	9.1 ± 0.5	13.4 ± 1.2
9	10	2395 ($L = 100$)	1347 ($L = 100$)	1.778	8.7 ± 0.5	12.7 ± 1.2
9	20	2430 ($L = 100$)	1367 ($L = 100$)	1.778	8.4 ± 0.9	12.1 ± 1.5

[a] The chain length is $L = 100$ except for one case ($L = 75$) of *spacing* $= 6$ and *distance* $= 3$. Just 10 000 samples are averaged to derive these results. The resulting entropy $S(16)$ is compared with $S(9)$ of the ordinary $F = 9 = 3 \times 3$ brush used in the other parts of this paper. The ratio $S(16)/S(9)$ should be compared with $16/9 = 1.778$ expected from the condition of extensive variable. The lateral linear dimensions, i.e., the mean-square distances of the center-of-mass vector $\sqrt{\langle x^2+y^2\rangle_g}$ and the end vector $\sqrt{\langle x^2+y^2\rangle_e}$, are listed in the sixth and seventh columns in units of lattice constant. If the polymers should not overlap themselves, these values should not be larger than the unit cell size, 9, 18, and 27 for *spacing* $= 3$, 6, and 9.

two polymer brushes consists of two parallel-oriented substrate planes and F (=18) polymer chains grafted on them, while the system of one polymer brush consists of only the lower substrate plane and F (=9) polymer chains grafted on it. Each chain is grown to their maximum length $L = 100$. The number of samples is typically 100 000 for each system.

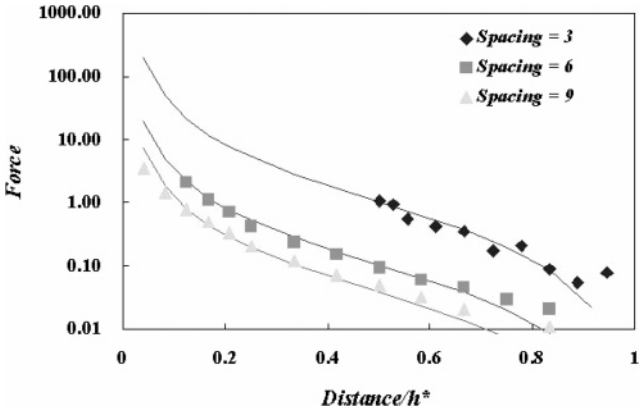

Figure 11. Semilogarithmic plot of the force as a function of *distance*/*h** in the case of a compressed polymer brush with *spacing* = 3, 6, and 9. The theoretical curves by MWC are also shown for comparison.

III. Results

(A) A Free Polymer Brush. We first consider the system of a free polymer brush as illustrated in Figure 3 and show the result. In Figure 4, the effective coordination number μ_l, which is related to the ratio of the total numbers of configurations, $N(l)/N(l-1)$, via eq 2, is plotted vs the length l of every chain; (a), (b), and (c) show the results of *spacing* = 4, 8, and 20, respectively. In every case, the values of μ_l are rather scattered for small l, reflecting the discreteness of the lattice, but lie always between 4 and 5. In the limit $l \to \infty$, μ's smoothly converge to the values 4.26, 4.55, and 4.66 for *spacing* = 4, 8, and 20, respectively. As *spacing* decreases, these values become significantly smaller than the ideal value 4.6838... that is expected for one isolated chain (self-avoiding walk) in a simple cubic lattice.[31] This means that the number of freedom is significantly reduced in the regime of high graft density. In the high-density limit, chains are most likely stretched in the direction perpendicular to the substrate plane.[4−7] Indeed, as seen from Figure 5 of the polymer density profile, the average height of the grafted polymers significantly increases as *spacing* decreases. In the case of highest graft density of *spacing* = 3, our numerical result for the density profile seems to obey particularly well the parabolic form

$$\rho(z) \sim \rho_0 - \alpha z^2 \tag{4}$$

of the MWC theory of the SCF approach in the high-density limit. The density profile for lower graft densities (*spacing* = 6, 9), however, does not fit so well to the parabolic form, but rather resembles the numerical result of the previous molecular dynamics simulation by Murat and Grest.[17]

Multiplying successively the ratios $N(l)/N(l-1) = \mu_l$ according to eq 3, we obtain the total number of configurations $N(L = 100)$ and in turn the entropy S for different values of *spacing*. The resulting entropy normalized by S_∞ at infinite *spacing* is shown in Figure 6. Obviously, it drops significantly when *spacing* becomes small, reflecting the fact that the number of freedom (i.e., the effective flexibility of the chains) is reduced. If we draw double-logarithmic plots for the entropy change $-\Delta S = S_\infty - S$ vs *spacing* (see Figure 7), we find a clear power-law decay of the entropy change

$$-\Delta S \sim (spacing)^{-x} \tag{5}$$

in the region of small *spacing*. The estimated exponent is $x = 2.4 \pm 0.1$. The derivative of eq 5 with respect to *spacing* gives the stress force proportional to $(spacing)^{-(x+1)}$ acting among polymer chains. This behavior of the stress force may be compared with the force between two boundary plates of a strip of polymer solutions $\sim 2R_g^2(L)/D^3$.[32] These behaviors seem qualitatively similar although the associated exponent is slightly different. This stress force is the origin of the cooperative soft and elastic behaviors of polymer brushes. Since it is purely an entropic force, polymer brushes with high graft density tend to be hard as the temperature increases.

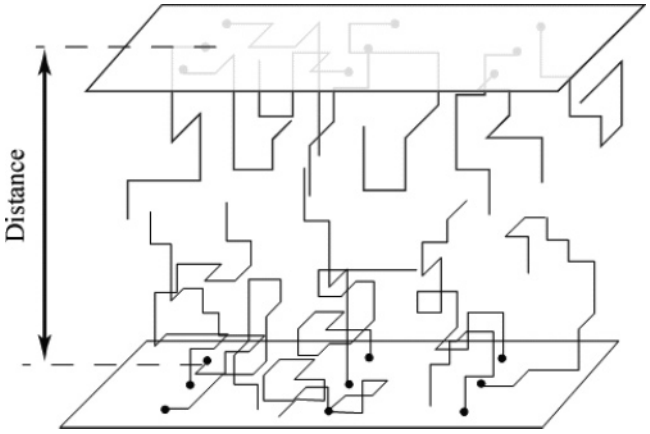

Figure 12. Schematic illustration of the system geometry of two polymer brushes facing each other. Here, "*distance*" denotes the distance between two substrate planes of the polymer brushes.

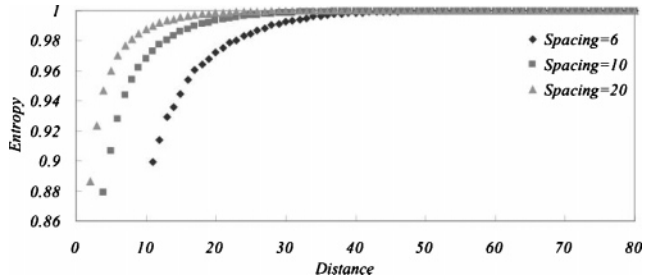

Figure 13. Entropy of the system of two polymer brushes facing each other. The ordinate is normalized by the entropy at infinite *distance*. The results for three systems with *spacing* = 6, 10, and 20 are shown.

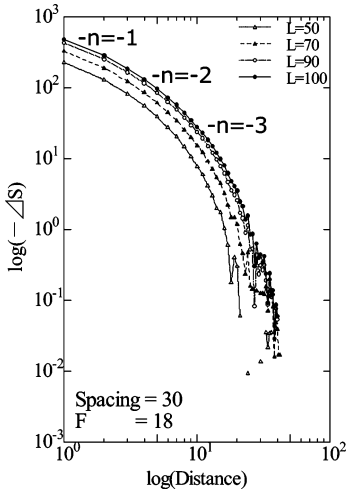

Figure 14. Double-logarithmic plot of the entropy change $-\Delta S$ as a function of *distance*. The slope of the curves does not correspond to any single exponent $-n$.

(B) A Compressed Polymer Brush. Next we consider the case where a polymer brush is compressed by a flat surface located in parallel to and with a "*distance*" from the brush substrate, as illustrated in Figure 8. Again, multiplying the ratios $N(l)/N(l-1)$ successively according to eq 3, we obtain the total

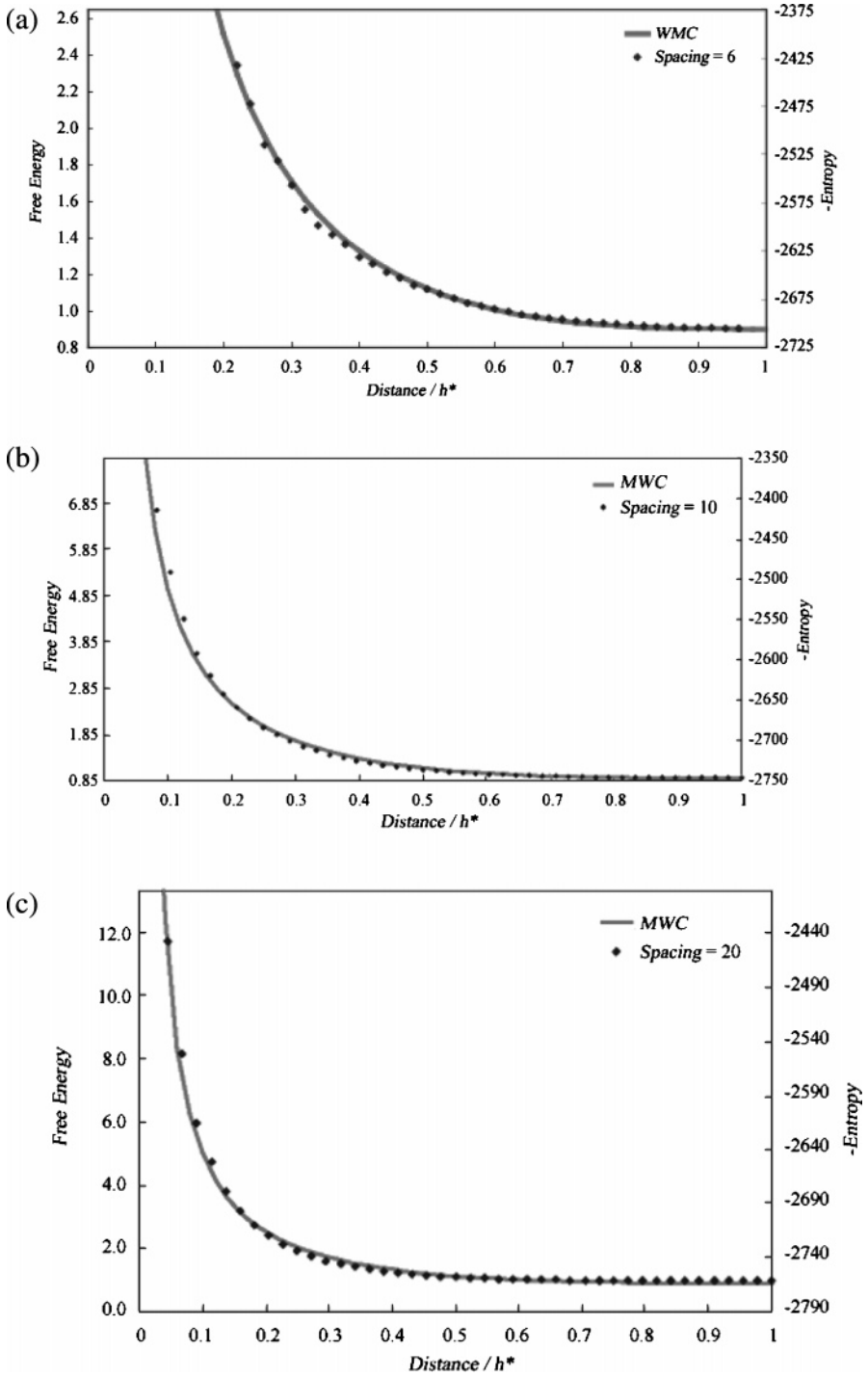

Figure 15. Comparison between the present result for the negative entropy (dots) and the MWC theory for the free energy (solid curves) in the case of two polymer brushes facing each other.

number of configurations $N(L = 100)$ and the entropy S. The resulting entropy normalized at infinite *distance* is depicted in Figure 9 for the systems of *spacing* = 3, 6, and 9. It is unity for large *distance* but decreases from unity as the *distance* approaches zero. The area of the depletion in the entropy near *distance* $\sim$ 0 is relatively small for *dpacing* = 3 but large for *spacing* = 9. As shown in Figure 10, the resulting entropy is well fitted by the theoretical free energy curves by the MWC theory eq 1 with $n = 1$. Here we have determined the equilibrium height h^* of the corresponding free polymer brush as a *distance* at which the entropy starts to drop in a compressed polymer brush; $h^* = 36$ for *spacing* = 3, $h^* = 24$ for *spacing* = 6, and $h^* = 24$ for *spacing* = 9. This agreement between our result and the MWC theory is quite excellent. The agreement is much better than the previous Monte Carlo result by Dickman and Anderson[22] and by Toral et al.,[23] who calculated the free energy by integrating the force. There is a clear difference between the results of ours and of these authors, although a possible difference might be attributed to the fact that our simulation directly estimates the entropy in the good solvent limit, while the simulations by these authors directly estimate the force nearly in good solvent.

Although the recent experiment by Yamamoto et al.[4,5] of the force profile is compared only with the scaling approach by de Gennes[11] in their paper, we find that their result agrees much better with our result and the result of the MWC theory than

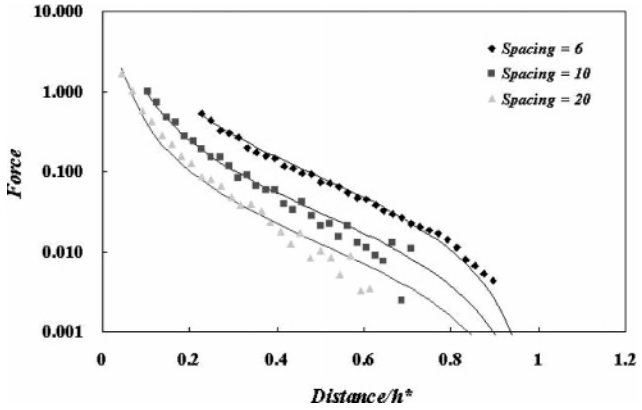

Figure 16. Semilogarithmic plot of the interlayer force vs *distance* between the two polymer brushes with *spacing* = 6, 10, and 20. The theoretical curves by MWC are also shown for comparison.

with the result of the scaling approach. Indeed, if we make a semilogarithmic plot of the force by taking the derivative of the entropy as a function of *distance* (see Figure 11), the result looks quite similar to Figure 7 of ref 4. In Figure 11, the solid curves are the MWC theory. The agreement between our result and the MWC theory is quite good except for the region of extremely small force around *distance*/$h^* \sim 1$. In this region, the logarithmic force depends linearly on *distance*/h^*, in excellent agreement with the experiment by Yamamoto et al.[4,5]

(C) Two Polymer Brushes. Finally, we consider the two polymer brushes facing each other (see Figure 12). Here, *distance* indicates the distance between two plates of the brush substrate surfaces. In this case, again we multiply the ratios $N(l)/N(l-1)$ successively according to eq 3 to obtain the total number of configurations $N(L = 100)$ and in turn the entropy S. We show the resulting entropy normalized at the infinite *distance* in Figure 13 for the systems with *spacing* = 6, 10, and 20. The entropy S drops significantly when the *distance* goes toward zero. This tendency becomes more significant when the chain length L increases. Figure 14 shows the double-logarithmic plot of the entropy change $-\Delta S(L,\textit{distance}) = S(L,\infty) - S(L,\textit{distance})$ vs *distance* for *spacing* = 30. In this case, however, we see that the data cannot be simply expressed by a power law with a single exponent $-n$. Instead, as shown in Figure 15, the entropy obeys very well eq 4 of the MWC theory with $n = 2$. Here also we have determined the equilibrium height h^* of the corresponding free polymer brush in the same way as the case of a compressed polymer brush as a *distance* at which the entropy starts to drop in the two facing polymer brushes; $h^* = 24$ for *spacing* = 6, $h^* = 24$ for *spacing* = 10, and $h^* = 22$ for *spacing* = 20. Here we notice that this behavior of the entropy change is quite different from that of two star polymers at a distance D[29]

$$\Delta S(D) \sim \alpha \log D \tag{6}$$

or that of a dilute polymer solution confined in a strip with a width D[32]

$$-\Delta S(D) \sim \frac{R_g^2(L)}{D^2} \tag{7}$$

Evaluating the derivative of the entropy S with respect to the plane *distance*, one may derive the interlayer force. Figure 16 shows the semilogarithmic plot of the interlayer force as a function of *distance* in the cases of *spacing* = 6, 10, and 20. From this figure, we find that the results nicely agree with the MWC theory, except for the region of extremely small force around *distance*/$h^* \sim 1$. We see that the force acts more like a cushion than a rigid wall. For small *distance*, the force fits well to the curve 1/(*distance*),[2] which is in accord with the experiments by Taunton et al.[3] and the Flory−Huggins mean-field theory.[3] Because of the lack of enough numerical accuracy of the present simulation, we cannot discuss the difference between the mean-field 1/(*distance*)^2 behavior and the scaling prediction 1/(*distance*)$^{9/4}$ due to de Gennes.[11] However, one may see that this short-distance behavior of the interlayer force is obviously different from the intermolecular force between two star polymers, α/*distance*,[29] or the interlayer force between the upper and lower plates of a strip (container) of polymer solutions, $2R_g^2(L)/(\textit{distance})^3$.[32]

IV. Discussion

It has been discussed in various papers[18,33] that the configuration of a chain in a brush is not cigarlike, as one might conclude from the Alexander picture,[10] but rather the lateral linear dimension in the directions parallel to the grafting surface scales like the square root of the chain length L. As a consequence, it must be expected that the chains (at least if L is large, such as $L = 100$) overlap themselves.

To check whether this is a problem, we analyzed a distribution function of the lateral components of the end-to-end vector as well as the vector from the grafting site to the center of mass of the chains. We also carried out several more simulations of a compressed polymer brush with larger number of polymers grafting on a substrate to check whether finite size effects invalidate the observables of interest. Although the necessary computational load increases exponentially as the number of polymers grafted on a substrate, we increased the number from $F = 9 = 3 \times 3$ to $F = 16 = 4 \times 4$ and carried out tentative simulations generating just 10 000 samples for several sets of *spacing* and *distance*. The chain length is $L = 100$, except for one case ($L = 75$) of *spacing* = 6 and *distance* = 3. The results are summarized in Table 1. It is found from this table that the entropies $S(16)$ and $S(9)$ for $F = 16$ and $F = 9$ scale linearly with the number of chains F because $S(16)/S(9)$ is very close to $16/9 = 1.778$ in every case. A possible error due to the finite size effect is 2% or less. This means that the finite size effect is negligible at least for the entropy.

On the other hand, the lateral linear dimension in the directions parallel to the grafting surface, the sixth and seventh columns of Table 1, is at most 6−9 and 10−13, respectively, for the center-of-mass and end vectors for every case. Regarding that the cell size is 9, 18, and 27 for *spacing* = 3, 6, and 9, respectively, we find that the chains do not overlap themselves seriously.

From these additional analyses, we conclude that our simulation using $L = 100$ chains with 3×3 cell size is valid.

V. Concluding Remarks

In this paper, we have carried out extensive numerical simulations of one and two polymer brushes swollen in good solvents by using the enrichment Monte Carlo algorithm on a simple cubic lattice. We have determined the entropy of free, compressed, and facing polymer brush systems and demonstrated that the excluded volume effect is essentially important in these properties. For a free polymer brush, we have found that the stress force between grafted polymers of a single polymer brush is qualitatively similar to the force between two boundary plates of the strip of polymer solutions[22] although the associated exponent is slightly different. On the other hand, for

a compressed polymer brush and for two polymer brushes facing each other, we have manifested that the MWC theory is fairly well satisfied. Moreover, for a compressed or two facing brushes, we have found that the resulting force agrees excellently well with previous experiments.[3−5] Its behavior is qualitatively different from the force between two star polymers[29] or between two boundary plates of the strip of polymer solutions.[32]

Although the present result on the interlayer force is in good agreement with previous experiments,[3−5] one should note that it is valid only at the thermal equilibrium. In the general case the systems may lie far off the thermal equilibrium. For example, if two polymer brushes are strongly compressed against the repulsive interaction and forced to come in a close proximity beyond the impenetrable region, then polymers are stuck and entangled. If we regard such entangled states as initial configurations, the story might change drastically because the entanglement effect makes the polymers stuck and immobile. This characterizes the sticky and adhesive property of the two polymer brushes facing each other. This is related to the sticking property of the so-called sticking polyhook straps, for example. Such a study would have another interest and must be considered in the future work.

Acknowledgment. The authors acknowledge the use of the HITACHI SR8000 supercomputer at the Computer Center of Hokkaido University. This work has been partly supported by the Grant-in-Aid for scientific research B (Grant No. 17310067) from Japan Society for the Promotion of Science (JSPS).

References and Notes

(1) Vincent, B. *Adv. Colloid Interface Sci.* **1974**, *4*, 193−77.
(2) Napper, D. H. *Polymeric Stabilization of Colloidal Dispersions*; Academic Press: London, 1983.
(3) Taunton, H. J.; Toprakcioglu, C.; Fetters, L. J.; Klein, J. *Macromolecules* **1990**, *23*, 571−580.
(4) Yamamoto, S.; Ejaz, M.; Tsujii, Y.; Matsumoto, M.; Fukuda, T. *Macromolecules* **2000**, *33*, 5602−5607.
(5) Yamamoto, S.; Ejaz, M.; Tsujii, Y.; Fukuda, T. *Macromolecules* **2000**, *33*, 5608−5612.
(6) Levicky, R.; Koneripalli, N.; Tirrell, M.; Satija, S. K. *Macromolecules* **1998**, *31*, 3731−3734.
(7) Anastassopoulos, D. L.; Vradis, A. A.; Toprakcioglu, C.; Smith, G. S.; Dai, L. *Macromolecules* **1998**, *31*, 9369−9371.
(8) Husseman, M.; Malmström, E. E.; McNamara, M.; Mate, M.; Mecerreyes, D.; Benoit, D. G.; Hedrick, J. L.; Mansky, P.; Huang, E.; Russell, T. P.; Hawker, C. J. *Macromolecules* **1999**, *32*, 1424−1431.
(9) Urayama, K.; Yamamoto, S.; Tsujii, Y.; Fukuda, T.; Neher, D. *Macromolecules* **2002**, *35*, 9459−9465.
(10) Alexander, S. *J. Phys. (Paris)* **1977**, *38*, 983.
(11) de Gennes, P. G. *J. Phys. (Paris)* **1976**, *37*, 1443. de Gennes, P. G. *Macromolecules* **1980**, *13*, 1069−1075. de Gennes, P. G. *Adv. Colloid Interface Sci.* **1987**, *27*, 189−209.
(12) Scheutjens, J.; Fleer, G. *J. Phys. Chem.* **1979**, *83*, 1619.
(13) Cosgrove, T.; Heath, T.; van Lent, B.; Leermakers, F.; Scheutjens, J. *Macromolecules* **1987**, *20*, 1692−1696.
(14) Muthukumar, M.; Ho, J. S. *Macromolecules* **1989**, *22*, 965−973.
(15) Milner, S. T.; Witten, T. A.; Cates, M. E. *Macromolecules* **1988**, *21*, 2610−2619.
(16) Zhulina, Y. B.; Pryamitsyn, V. A.; Borisov, O. V. *Polym. Sci. U.S.S.R.* **1989**, *31*, 205−216.
(17) Murat, M.; Grest, G. S. *Macromolecules* **1989**, *22*, 4054−4059.
(18) Murat, M.; Grest, G. S. *Phys. Rev. Lett.* **1989**, *63*, 1074−1077.
(19) Lai, P.-Y.; Binder, K. *J. Chem. Phys.* **1991**, *95*, 9288−9299.
(20) Lai, P.-Y.; Binder, K. *J. Chem. Phys.* **1992**, *97*, 586−595.
(21) Lai, P.-Y.; Binder, K. *J. Chem. Phys.* **1993**, *98*, 2366−2375.
(22) Dickman, R.; Anderson, P. E. *J. Chem. Phys.* **1993**, *99*, 3112−3118.
(23) Toral, R.; Chakrabarti, A.; Dickman, R. *Phys. Rev. E* **1994**, *50*, 343−348.
(24) Kreer, T.; Metzger, S.; Müller, M.; Binder, K. *J. Chem. Phys.* **2004**, *120*, 4012−4023.
(25) Kreer, T.; Müser, M. H.; Binder, K.; Klein, J. *Langmuir* **2001**, *17*, 7804−7813.
(26) Ohno, K.; Binder, K. *J. Stat. Phys.* **1991**, *64*, 781−806.
(27) Ohno, K. *Macromol. Symp.* **1994**, *81*, 121−127.
(28) Ohno, K.; Schulz, M.; Binder, K.; Frisch, H. L. *J. Chem. Phys.* **1994**, *101*, 4452−4460.
(29) Ohno, K.; Shida, K.; Kimura, M.; Kawazoe, Y. *Macromolecules* **1996**, *29*, 2269−2274.
(30) Shida, K.; Ohno, K.; Kimura, M.; Kawazoe, Y. *Comput. Theor. Polym. Sci.* **2000**, *10*, 281−285.
(31) Watts, M. G. *J. Phys. A: Math. Gen.* **1975**, *8*, 61−66.
(32) de Gennes, P. G. *Scaling Concepts in Polymer Physics*; Cornell University Press: Ithaca, NY, 1979.
(33) Wittmer, J.; Johner, A.; Joanny, J. F.; Binder, K. *J. Chem. Phys.* **1994**, *101*, 4379−4390.

MA0613234